Title	Design method for micromixers considering influence of channel confluence and bend on diffusion length
Author(s)	Aoki, Nobuaki; Umei, Ryota; Yoshida, Atsufumi; Mae, Kazuhiro
Citation	Chemical Engineering Journal (2011), 167(2-3): 643-650
Issue Date	2011-03
URL	http://hdl.handle.net/2433/157340
Right	© 2010 Elsevier B.V.
Type	Journal Article
Textversion	author

Original Paper

Design method for micromixers considering influence of channel confluence and bend on diffusion length

Nobuaki Aoki, Ryota Umei, Atsufumi Yoshida, Kazuhiro Mae[*]

Department of Chemical Engineering, Graduate School of Engineering, Kyoto University, Kyoto-daigaku Katsura, Nishikyo-ku, Kyoto 615-8510, Japan

*Corresponding author. Tel.: +81 75 383 2668; fax: +81 75 383 2658.

E-mail address: kaz@cheme.kyoto-u.ac.jp (K. Mae).

Abstract

In micromixers, fluids deform through convection generated by variations in the shape of a channel, e.g., channel confluence and bend. This deformation enhances the mixing performance of the micromixer. In this study, we consider the effect of deformation on mixing performance in terms of a reduction in diffusion length, which is equivalent to the size of the fluid segments formed through fluid deformation. Based on improvements in the mixing rate through convection, we establish a design method that enables a micromixer to achieve a desired rapid mixing rate. For this purpose, we correlate the mixing performance of micromixers having various channel shapes and fluid velocities with the diffusion length; the equivalent mixing rate is obtained using computational fluid dynamics (CFD) simulations. The results of the CFD simulations reveal that the combination of fluid collision and channel bend after the development of the velocity profile of confluent flow is effective at enhancing the mixing rate. To establish a design method for a micromixer, we define and employ the energy dissipation rate based on the pressure drop profile in microchannels. The relationship between the segment size and the energy dissipation rate based on channel shape has been derived and integrated into the design method.

Keywords: Micromixer; Diffusion length; Energy dissipation rate; Collision; Bend; Computation Fluid Dynamics

1. Introduction

Microreactors are miniaturized reactors that have microchannels of characteristic dimensions in the submillimeter range [1]. Some micromixers, which are mixers containing submillimeter mixing chambers, can be used as a reactor especially for reactive mixing. The reactor miniaturization provides improved mass- and heat-transfer rates and thus enables us to proceed with reactions under conditions controlled more precisely as compared to conventional macro-scale reactors, which leads to the possibility of improved yields and selectivities of desired products [2]. Enhancing mixing performance in microreactors is also essential to produce desired products in high yield and selectivity by precisely controlling reactor operations. The selectivities of desired products for very fast multiple reactions have been improved using micromixers, which are miniaturized mixing devices [3]. Micromixers are, thus, important components of microreactors used to control reactor operations. Many mixing principles have been developed for enhancing mixing performance in micromixers [4]. Many other principles have been derived by focusing on reducing the diffusion length between reactants. This is because mixing in microreactors is mainly driven by molecular diffusion and reactor miniaturization leads to low Reynolds numbers in reactor channels. In micromixers, splitting reactant fluids into small fluid segments is a method to reduce diffusion length and thus enhance mixing performance. Three principles are mainly used to split reactant fluids into small fluid segments. The first principle is to divide reactant fluids into

many fluid segments using the channel geometry of micromixers. One mixing method that uses this mixing principle splits reactant fluids into many laminated fluid segments by the geometry of the inlet channels that lead into the mixing chamber. Examples of micromixers using this mixing method include the interdigital mixer [5] and the multi-stream mixer with focusing after confluence [6,7]. When only this mixing principle is used, it is necessary to shorten the diffusion length by channel reduction to achieve fast mixing. However, channel reduction also leads to a high-pressure drop in the channel and thus a limited flow rate, resulting in a low productivity and operability. Another principle that enhances mixing performance is therefore needed for industrial production where high throughput is to be achieved.

The second principle used to split reactant fluids into small fluid segments is the collision of reactant fluid streams by applying shear to the streams. The collision deforms fluids and shortens the diffusion length between the fluids. As a result, the mixing performance is improved. To evaluate the mixing rate quantitatively, we can consider the enhancement of mixing performance in terms of a reduction in diffusion length (fluid segment size). Collision of two fluid streams at a channel confluence is the simplest method for this mixing principle. T- and Y-shape microchannels are examples of micromixers that use this mixing principle and have been employed in investigations on the relationship between design factors such as channel sizes and flow rates in the mixers, flow pattern, and mixing

performance in the micromixers [8–10].

The third principle commonly applied is channel bend. Channel bend also deforms fluids and shortens the diffusion length between fluids. Previous investigations based on experimental and simulation results reveal that channel shapes of bend and curve after fluid collision enhance mixing performance [11,12].

However, most previous investigations considered only the qualitative effects of channel shape on mixing. For the versatile use of micromixers in industrial production, a method to design channels in accordance with the kinetics of the reaction system is needed. Quantitative relationships between mixing rate and design parameter of microchannels utilizing convection are required for this purpose. In this context, we correlate the mixing performance of microchannels having various channel shapes and fluid velocities with the diffusion length, which gives the equivalent mixing rate using computational fluid dynamics (CFD) simulations. To establish a design method, we also propose an index to express the effects of both channel shapes and operating conditions on mixing performance and integrate the index into the design method.

2. Simulation Method

2.1 Geometry of microchannels

The three-dimensional laminar flow and the finite-rate model of Fluent 6.3 were used in the CFD simulations. We simulated mixing between fluids A and B having the same physical properties with each inlet velocity v in the microchannels. Table 1 lists the physical properties of fluids A and B.

As explained in the introduction, mixing can be enhanced by convection due to channel confluence and bend. To examine the effects of channel shapes on mixing rate, we simulated various sizes of microchannels with combinations of channel confluence and bend. Figs. 1 (a) and (b) show schematics of micromixers that include these channel shapes. The micromixer containing only channel confluence is called the Tmixer and the mixer with both channel confluence and bend is referred to as the TLmixer. The channel sizes d_x, d_y, and d_z [μm], and the channel length between the points for channel confluence and bend X [mm] and bend angle θ [degree] are considered as design parameters. In the simulations, the relationship among the channel sizes was fixed as $d_x = d_z = d_y/2$.

Table 2 lists the micromixers used in this investigation. The mixer names represent the design parameters. We name micromixers using the shape of mixer (T or TL), the channel hydraulic diameter D, the channel length between the points of channel confluence collision and channel bend, and the bend angle. The definition of D is given by

$$D = \frac{2d_x d_y}{d_x + d_y} \tag{1}$$

The TLmixers include a bend of 90° at X = 1 mm after the channel confluence (see Fig. 1(b)

for the definition of the length of *X*). The TL-*X*mixers include a bend of 90° at *X* mm after the collision. In the T-θmixers, the channel bends with an angle of θ at 1 mm after the collision. Therefore, TL133 and TL133-90° have the same shape, and TL167 and TL167-1 also have the same shape.

The intensity of convection depends on the inlet velocity. For this reason, we considered the inlet velocity to be a design parameter and investigated the effects of velocity on mixing enhancement for each shape. The range of inlet velocity v is between 0.6–2 m/s, and the corresponding Reynolds number is between 120–300.

In addition, we simulated mixing in a multi-lamination mixer (MLmixer). In the MLmixer, the flow rate is so low that only molecular diffusion promotes mixing. Under such conditions, the mixing rate in the MLmixer depends on the fluid segment size W [μm], namely the diffusion length. As shown in Fig. 1 (c), the multi-lamination of fluids in the ML mixer is expressed by periodic boundaries in the width and depth directions. For the Tmixer and TLmixer, each fluid deforms through channel confluence and channel bend as shown in Fig. 2. We considered the effect of this deformation in terms of a reduction in diffusion length. By obtaining the MLmixer fluid segment size, which gives the corresponding mixing rate for the Tmixer or TLmixer, we can quantify the enhancement in mixing achieved through channel confluence and bend in terms of a reduction in the diffusion length W.

2.2 Evaluation of mixing performance

We evaluate the degree of mixing in a plane perpendicular to the axial direction of the microchannel using the mixing ratio δ. The definition of δ is given by

$$\delta = \sigma/\sigma_0 \tag{2}$$

where σ is the standard deviation of the mass fraction of A in a plane perpendicular to the axial direction and σ_0 is the initial standard deviation. The value of σ is obtained from the mass fraction of A for each calculating cell in the designated plane. The standard deviation is calculated by the following equation:

$$\sigma = \sqrt{\frac{\sum_{i=1}^{n} A_i \left(m_i - \overline{m}\right)^2}{A_{\text{total}}}} \tag{3}$$

where m_i is the mass fraction of A in each cell, $\overline{m}$ is the mean mass fraction of A for all cells in the plane, A_i is the area of calculating cell i in the designated plane, and A_{total} is the total area of the calculating zone, and n is the number of cells in the plane. Before mixing, the value of δ is 1 ($\sigma = \sigma_0$). Reaching $\delta = 0$ means that the mixing is complete, since the mass fraction is uniform and the deviation reaches zero. Fig. 2 shows an example of the change in the mass fraction profile and corresponding values of δ in a microchannel. The relationship between the mixing ratio and the mean residence time is obtained by calculating δ for several planes of axial positions in each microchannel. The mean residence time for a plane

perpendicular to the axial direction in a microchannel is calculated from the distance of the plane from the point right after the channel confluence divided by the total fluid velocity.

2.3 Discretization method for CFD simulations

The employed CFD code, Fluent, solves for the mass, momentum, and component conservation equations using the control volume method [13]. To solve conservation equations, we employed the first-order upwind difference scheme for momentum, and the second-order upwind difference scheme for each component. The Semi-Implicit Method for Pressure-Linked Equations (SIMPLE) algorithm was used to solve the pressure-velocity coupling equation. In the CFD simulations, we defined a floating-point number as single precision. The calculation domain was discretized using the following shapes of cell and the numbers of cell elements. The physical size of each cell was 4 μm, with the exception of TL67, which had a cell size of 2 μm. The cell shapes are nearly cubical hexahedrons, and the number of cells for each simulation is approximately 1.8 million.

3. Results and Discussion

3.1 Comparison of mixing performance of Tmixer and TLmixer

To extract the relationship between the channel shape and the mixing rate, the mixing ratio of the Tmixer or TLmixer is correlated to that of the MLmixer. Fig. 3 shows the influence of channel shape on the mixing ratio over the mean residence time, τ, for various inlet velocities of T167 and TL167. The TLmixer has a better mixing performance because of the combination of channel confluence and bend. However, after τ = 2 ms, the mixing ratio gradually decreases. This tendency means that mixing is mainly driven by molecular diffusion, and not by convection. With this result, to extract the convection effects based on the channel shapes, we defined the mixing rate of Tmixer, TLmixer, and MLmixer using $\delta_{2\mathrm{ms}}$ (the mixing ratio at τ = 2 ms). For example, we can read $\delta_{2\mathrm{ms}}$ = 0.85 in T167-1 m/s from Fig. 3. Then, Fig. 4 shows the relationship between $\delta_{2\mathrm{ms}}$ and the fluid segment size for the MLmixer, W. Owing to no convection effect, the fluid segment size for the MLmixer is equivalent to the diffusion length. The value of $\delta_{2\mathrm{ms}}$ of the MLmixer with W = 17 μm is 0.85. Therefore, the mixer T167-1 m/s gives the equivalent mixing rate of the MLmixer with W = 17 μm, which is smaller than 83.5 μm, that is, the fluid segment size originated from the channel size of the mixer T167 (half of the channel size after confluence). In other words, we can consider that the mixing enhancement obtained through channel confluence and bend corresponds to the reduction in the diffusion length. Hereafter, we call the fluid segment size giving the

equivalent mixing rate the “effective fluid segment size” and consider that the size is the measure of the mixing rate of each microchannel. By searching for the W of the ML mixer that yields an equal δ_{2ms} value of a microchannel, the effective fluid segment size of the channel can be obtained. In this way, we correlate the δ_{2ms} of the Tmixer or TLmixer to that of the MLmixer to extract the relationship between the channel shape and the mixing rate. Note that in reality, the fluid segments in the microchannels producing the convection effect have fuzzy shapes and that the assumption of a well defined and uniform “fluid segment size” is just a model assumption used in the mixing performance evaluation and in a design procedure that is established later.

3.2 Derivation of an index for relating mixing performance and design parameters

As described in the previous section, we first correlated the fluid segment size W and the mixing ratio δ_{2ms} using the MLmixer. In addition to this correlation, we needed to determine the relationship between the mixing ratio δ_{2ms} and the design parameters D and v to establish a design method for a micromixer. In this section, we propose an evaluation index of mixers.

3.2.1 Reynolds number

For various investigations of micromixers, the mixing performance has been correlated using Reynolds number [14,15]. The Reynolds number is defined based on the channel hydraulic diameter of the channel after fluid collision *D* and is defined in Eq. (1)

$$Re = \frac{Dv\rho}{\mu} \tag{3}$$

where *v* is the inlet velocity of fluid in channels. Fig. 5 shows the relationship between the effective fluid segment size and the Reynolds number. At the same Reynolds number, the fluid segment size of the TLmixer is shorter than that of the Tmixer because of mixing enhancement through the channel bend. From this result, we conclude that the fluid segment size depends on only the Reynolds number when the shape is fixed. Using this figure, we can relate the fluid segment size and the design parameters. However, the Reynolds number is constant even if the bend angle varies. For this reason, the Reynolds number cannot independently express the effects of this angle on the mixing rate. To integrate the effects of bend angle in the design method of a micromixer, another index that relates channel shape, design parameters, and mixing performance is required.

3.2.2 Energy dissipation rate

Mixing performance is enhanced by channel bend and fluid collision through channel confluence because the fluid energy is dissipated and convection arises in these shapes. In this context, we focus on the energy dissipation rate to coordinate mixing performance through channel confluence and bend. Matsuyama et al. have proposed the expression of the energy dissipation rate as follows:

$$\varepsilon = \frac{Q \Delta P}{\rho V} \tag{4}$$

where Q is the volume flow rate, ΔP is the arbitrary pressure drop in the focused space, and V is the volume of the focused space [16,17]. Since the value of ε is a spatial average, it depends on the focused space. Therefore, we can define the energy dissipation rate when we determine a spatial volume where convection arises and compute the pressure drop in the space. The energy dissipation is also expressed by residence time as follows:

$$\varepsilon = \frac{\Delta P}{\rho \tau} \tag{5}$$

To obtain a large energy dissipation rate, not only a large pressure drop, but also a large variation in pressure per time is desired. In microchannels, a residence time of the order of milliseconds can be chosen. Therefore, we can obtain a large energy dissipation rate in the microchannels.

We focus on the pressure distribution and the mass fraction distribution in channels to determine the volume of the focused space V. This is because the gradient of the pressure drop is large in the space where convection dominates mixing. In this space, the interfacial

geometry between fluids deforms through the convection. For example, Fig. 6 shows the static pressure in the channel after fluid collision in TL167. We define the plane right after channel confluence as L = 0 mm and the plane of right before the channel bend as L = 1 mm. We set the pressure at the channel outlet at 0 kPa as the reference. The gradients of pressure drop for the volume denoted by the circles in Fig. 6 are large because these points correspond to the pressure gradients just after channel confluence and bend. Fig. 7 shows the change in the mass fraction profile inside of TL167. The interfacial geometry also deforms just after channel confluence and bend. From these figures, we confirm that the space where the gradient of the pressure drop is large corresponds to that where interfacial geometry deforms. After the channel bend, the interfacial geometry remains unchanged, and diffusion dominates mixing.

On the basis of the results shown above, we determined the channel after fluid collision and channel bend as the focused space where convective flow drives mixing. From the simulation results of various design parameters, we find that the volume of space is equal to 2D after channel confluence and bend, respectively. We define the sum of the space as the focusing volume. As shown in Fig. 8, V_1 and V_2 are the volumes of post-channel confluence and bend, respectively. ΔP_1 and ΔP_2 are the pressure drops of post-collision and bend, respectively. Using these parameters, we define the energy dissipation rate as follows:

$$\varepsilon = \frac{Q\left(\Delta P_1 + \Delta P_2\right)}{\rho\left(V_1 + V_2\right)} \tag{6}$$

Fig. 9 shows the relationship between the effective fluid segment size and the energy dissipation rate. In the low flow rate range, the relationship depends on D because molecular diffusion dominates mixing. In contrast, strong convection dominates mixing in the high flow rate range, and the fluid segment size decreases approximately 5 μm at D = 133–200 μm if $\varepsilon \geq 10^4$ W/kg. In the range of $\varepsilon \geq 10^4$ W/kg, the effective fluid segment size asymptotically decreases. This size is of the order of the Kolmogorov length λ defined by

$$\lambda = \left(\frac{\nu^3}{\varepsilon} \right)^{1/4} \tag{7}$$

where ν is the kinematic viscosity of fluid A and B [m^2/s] [18]. In this investigation, λ = 3.2 μm for $\varepsilon = 10^4$ W/kg. From the Reynolds number, the flow in the straight channel is laminar. However, the fluid is irregularly deformed at the channel confluence and bend. We infer that the turbulence effect may affect the mixing rate at these points. For TL200 with $\varepsilon \geqq 10^4$ W/kg, the diffusion length is originally 100 μm at the channel confluence, and it becomes 5 μm after only 2 ms. In other words, the shapes of channel confluence and bend have the same effect as splitting the fluids into 20 identical fluid segments using parallel channels and then contacting the segments. To quantify the effect of the diffusion length reduction through channel confluence and bend, we introduce the split number n defined by

$$n = \frac{D/2}{W} = \frac{D}{2W} \tag{8}$$

From this definition, the value of n is equal to 20 for TL200 with $\varepsilon \geqq 10^4$ W/kg. Fig. 10 shows the relationship between energy dissipation rate and the split number n. For large

values of ε, the value of n is greater than 10. If fluid segments of such numbers are produced by only channel geometry, small channels are required, which results in a large pressure drop in the micromixers. Thus, the shapes of channel confluence and bend are effective to enhance mixing performance without reducing the operability of micromixers.

3.3 Influence of distance X between points of channel confluence and bend

To determine the influence of distance X between collision and bend on the mixing rate, we considered the results of a simulation of TL167-X. Fig. 11 shows the mixing ratio as a function of distance from the point of channel confluence for T167 and TL167-X. The value of X is 0.1, 0.2, 0.33, 0.5, 1, and 2 mm. For TL167-X, the bend shape enhances mixing performance if $X \geqq 0.5$ mm.

We identified the range of X that enhances the mixing performance based on the entrance length L_e. The entrance length is the distance required for the centerline velocity to reach 99 % of the fully developed velocity after a flow enters a narrow channel. The length is given by the following equation [19]:

$$L_e/D = 0.379\exp(-0.418\,Re) + 0.0550\,Re + 0.260 \quad (9)$$

This equation is valid for the range of $0 < Re < 500$, and in this case (D = 167 μm, Re = 133), the length is 1.3 mm. From the results shown in Fig. 11, the bend shape enhances mixing

performance if $X \geqq L_e/3$. We also confirmed this tendency for the microchannels listed in Table 2. With these results, we chose X = 1 mm to fully utilize the bend shape effect.

3.4 Influence of bend angle θ

To identify the effect of bend angle θ on mixing performance, we considered the results of a simulation of T133-θ. Fig. 12 shows the effective fluid segment size as the mixing performance index against the energy dissipation rate for T133-θ. The value of the bend angle θ is 30°, 60°, 90°, and 120°. The curves of these angles fit well, and the fluid segment size depends on only the energy dissipation rate with a fixed channel size.

When the energy dissipation rate is fixed, a large bend angle requires a small inlet velocity. That is, the pressure drop in the channel after the bend decreases with increasing bend angle. Under the limitation of space in the layout of the channels, the largest applicable bend angle is desired.

To develop a design method for a micromixer, we then formulated the energy dissipation rate theoretically using Eq. 4. In laminar flow, the pressure drop in a channel consists of ΔP_f and ΔP_c. ΔP_f is the pressure drop of friction between the fluid and channel wall, whereas ΔP_c is the pressure drop of convection by channel confluence or bend.

$$\Delta P = \Delta P_f + \Delta P_c = 4f\left(\frac{L}{D}\right)\left(\frac{\rho v^2}{2}\right) + \xi\frac{\rho v^2}{2} = f^*\frac{L}{D}\rho v^2 \tag{10}$$

where f is the friction factor [-], and ξ is the friction loss factor that depends on channel shapes such as contraction, expansion, bifurcation, collision, bend, and orifice [-]. We define the overall friction factor f^*, which includes friction effects in the straight channel and the shapes of channel confluence and bend.

$$f^* = 2f + \zeta \frac{D}{2L} \tag{11}$$

Substituting the pressure drop of Eq. (4) with Eq. (10), the energy dissipation rate is formulated using the inlet velocity and the channel hydraulic diameter.

$$\varepsilon = \frac{d_x d_y \cdot v \cdot f^* \left(\frac{L}{D} \right) \rho v^2}{\rho \cdot L d_x d_y} = f^* \frac{v^3}{D} \tag{12}$$

Fig. 13 shows the relationship between the energy dissipation rate established by simulation and the corresponding v^3/D. From the slop of this figure, we obtain the value of f^* for each bend angle. We then correlate f^* with θ, and the relationship for TL133 is, for example, determined as follows:

$$f^* = 0.0011 \times \theta + 0.2128 \tag{13}$$

For different channel sizes, the same procedure can be applied. Using Eqs. (6) and (13), the energy dissipation rate is expressed by the design parameters.

3.5 Design procedure for micromixer

Using the results described in the previous sections, we establish a design

procedure for a micromixer. First, we explain the method to determine the factors that we have not discussed yet. From the reaction kinetics, the mixing rate and the effective fluid segment size W (diffusion length) required to achieve a reaction-controlled condition are determined. For this purpose, we can use a threshold value of Damköhler number, which is the ratio of the mixing rate to the reaction rate [20]. When the value of the dimensionless number for a reactor operation is smaller than the threshold value, the reaction proceeds under a reaction-controlled condition. The fluid segment shape and size for achieving the threshold value has been investigated in our previous papers [21−23]. Moreover, if the reaction is exothermic, the yield and selectivity of the desired products depend on heat transfer. Therefore, we can determine the heat transfer rate that maximizes the yield and selectivity. To achieve the desired heat transfer rate, the specific surface area and corresponding channel hydraulic diameter D is specified. Summarizing the discussion in the previous sections and above, a design procedure for a micromixer satisfying the design conditions is described as follows, and Fig. 14 illustrates the procedure.

1. The effective fluid segment size W is determined from the reaction kinetics and the channel hydraulic diameter D is determined from the required heat transfer rate as design parameters.
2. Using the relationship between W and the energy dissipation rate ε, the required value of ε is specified.

3. From the limitation of the configuration of channels surrounding the micromixer, the bend angle θ is determined.
4. Using Eq. (12), the inlet velocity v is specified.
5. Using the equation of entrance length, the distance between the points of channel confluence and bend X is determined.

4. Conclusion

In this study, the effects of microchannel shapes such as channel confluence and bend on mixing performance have been intensively examined. Through this study, we found that the combination of channel confluence and bend gives a better mixing performance. This effect is valid when the channel bend is set after the confluent flow has fully developed. To develop a design method for a micromixer, we first express the enhancement in mixing rate through these shapes using the fluid segment size, which is correlated to the diffusion length in a multi-lamination mixer. In the multi-lamination mixer, the laminated fluid segment width is equal to the diffusion length. Then, the relationship between the correlated segment size and the energy dissipation rate based on the pressure drop in a space where convention dominates mixing is derived. With a fixed channel size, the mixing performance depends only on the bend angle. Using these relationships, we have established a design method for a

microchannel that considers channel confluence and bend for achieving reaction-controlled conditions. Establishing such design methods leads to the development of a systematic approach to developing microreactors. Such an approach is important to enable the universal use of microreactors in industrial processes.

Acknowledgements

This research was supported by the New Energy and Industrial Technology Development Organization (NEDO) through the Project of Development of Microspace and Nanospace Reaction Environment Technology for Functional Materials.

References

[1] V. Hessel, S. Hardt, H. Löwe, Chemical Micro Process Engineering, WILEY-VCH, Weinheim, Germany, 2004.

[2] H.S. Fogler, Elements of Chemical Reaction Engineering, 4th ed., Pearson Education, Upper Saddle River, USA, 2005, pp. 201–207.

[3] W. Ehrfeld, V. Hessel, H. Löwe, Microreactors, New Technology for Modern Chemistry, Wiley, New York, 2000, pp. 144–164.

[4] V. Hessel, H. Löwe, F. Schönfeld, Micromixers—a review on passive and active mixing principles, Chem. Eng. Sci. 60 (2005) 2479–2501.

[5] W. Ehrfeld, K. Golbig, V. Hessel, H. Löwe, T. Richter, Characterization of mixing in micromixers by a test reaction: single mixing units and mixer arrays, Ind. Eng. Chem. Res. 38 (1999) 1075–1082.

[6] P. Löb, K.S. Drese, V. Hessel, S. Hardt, C. Hofmann, H. Löwe, R. Schenk, F. Schönfeld B. Werner, Steering of liquid mixing speed in interdigital micro mixers – from very fast to deliberately slow mixing, Chem. Eng. Technol. 27 (2004) 340–345.

[7] Y. Wang, Q. Lin, T. Mukherjee, A model for laminar diffusion-based complex electrokinetic passive micromixers, Lab Chip 5 (2005) 877–887.

[8] W.D. Mohr, R.L. Saxton, C.H. Jepson, Mixing in laminar-flow systems, Ind. Eng. Chem. 49 (1957) 1855–1856.

[9] M. Engler, N. Kockmann, T. Kiefer, P. Woias, Numerical and experimental investigations on liquid mixing in static micromixers, Chem. Eng. J. 101 (2004) 315–322.

[10] D. Gobby, P. Angeli, A. Gavriilidis, Mixing characteristics of T-type microfluidic mixers, J. Micromech. Microeng. 11 (2001) 126–132.

[11] N. Kockmann, T. Kiefer, M. Engler, P. Woias, Convective mixing and chemical reactions in microchannels with high flow rates, Sens. Act. B 117 (2006) 495–508.

[12] W. Jeon, C.B. Shin, Design and simulation of passive mixing in microfluidic systems with geometric variations, Chem. Eng. J. 152 (2009) 575–582.

[13] Fluent 6.3 User's Guide, Fluent Inc., Lebanon, USA, 2006, pp. 25-2–25-47.

[14] S. Panic, S. Loebbecke, T. Tuercke, J. Antes, D. Boskovic, Experimental approaches to a better understanding of mixing performance of microfludic devices, Chem. Eng. J. 101 (2004) 409–508.

[15] M.-A. Schneider, T. Maeder, P. Ryster, F. Stoessel, A microreactor-based system for the study of fast exothermic reactions in liquid phase: characterization of the system, Chem. Eng. J. 101 (2004) 241–250.

[16] S. Middleman, Drop size distributions produced by turbulent pipe flow of immiscible fluids through a static mixer, Ind. Eng. Chem. Proc. Des. Dev. 13 (1974) 78–83.

[17] K. Matsuyama, K. Mine, H. Kubo, N. Aoki, K. Mae, Optimization methodology of operation of orifice-shaped micromixer based on micro-jet concept, Chem. Eng. Sci., in press.

[18] J. Baldyga, R. Pohorecki, Turbulent micromixing in chemical reactors - a review, Chem. Eng. J. 58 (1995) 183–195.

[19] N. Dombrowski, E.A. Foumeny, S. Ookawara, A. Riza, The influence of Reynolds number on the entry length and pressure drop for laminar pipe flow, Can. J. Chem. Eng. 71 (1993) 472–476.

[20] E.L. Paul, V.A. Atiemo-Obeng, S.M. Kresta, Handbook of Industrial Mixing: Science and Practice, John Wiley & Sons, Hoboken, USA, 2004, p. 33.

[21] N. Aoki, S. Hasebe, K. Mae, Mixing in microreactors: effectiveness of lamination segments as a form of feed on product distribution for multiple reactions, Chem. Eng. J. 101 (2004) 323–331.

[22] N. Aoki, S. Hasebe, K. Mae, Geometric design of fluid segments in microreactors using dimensionless numbers, AIChE J. 52 (2006) 1502–1515.

[23] N. Aoki, K. Mae, Nonisothermal design of fluid segments for precise temperature control in microreactors, Chem. Eng. Sci. 63 (2008) 5035–5041.

List of table and figure captions

Fig. 13. Plots of ε against v^3/D used to obtain f^*.

Fig. 14. Design procedure for micromixer.

Table 1

Physical properties of fluids A and B

Density, ρ	1.0×10^{3}	kg/m^3
Viscosity, μ	1.0×10^{-3}	Pa·s
Diffusivity, D_{AB}	1.0×10^{-9}	m^2/s

Table 2

Design parameters of micromixers employed in CFD simulations

shape	notation	X [mm]	θ [degree]
Tmixer	T133, 167, 200	-	-
TLmixer	TL67, 133, 167, 200	1	90
TL-Xmixer	TL167-0.1, 0.2, 0.33, 0.5, 1, 2	X	90
T-θmixer	TL133-30°, 60°, 90°, 120°	1	θ

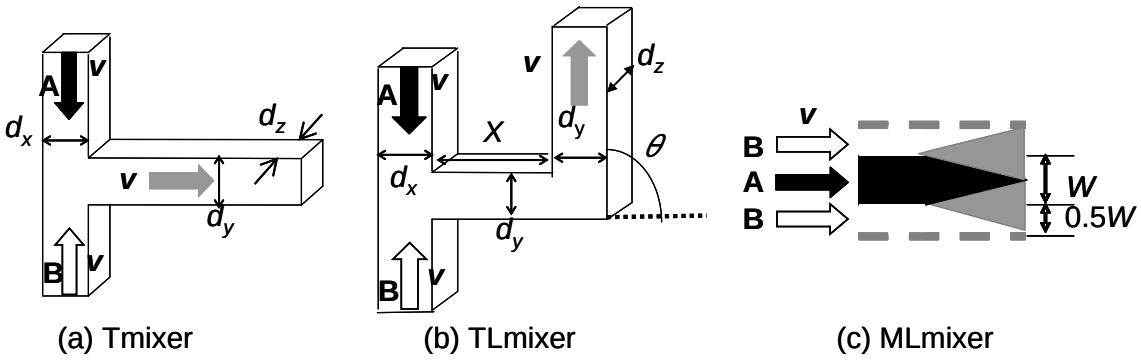

Fig. 1. Schematic of micromixers. (a) Tmixer, (b) TLmixer, and (c) MLmixer.

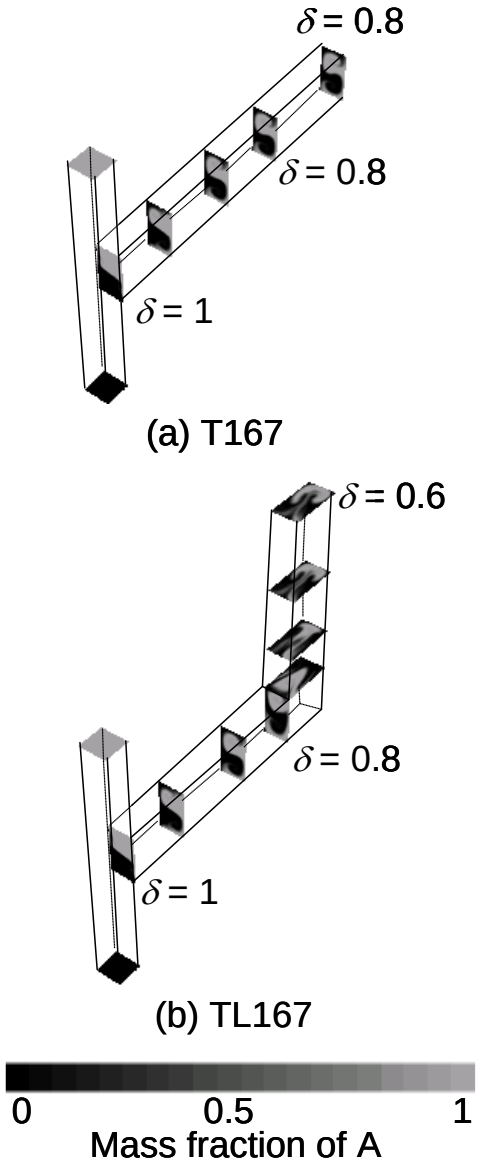

Fig. 2. Example of change in mass fraction profile in microchannel. (a) T167 (v = 1 m/s) and (b) TL167 (v = 1 m/s).

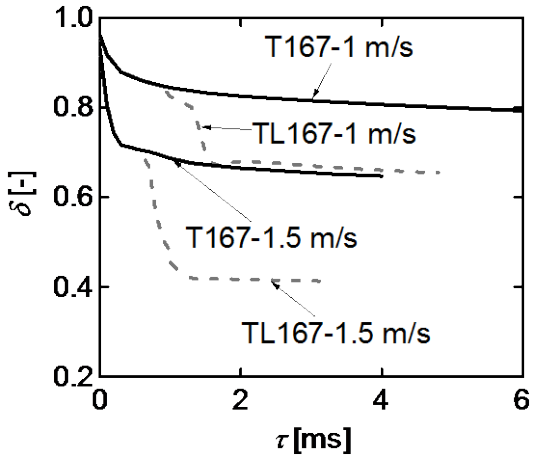

Fig. 3. Influence of channel shape on mixing ratio over mean residence time τ.

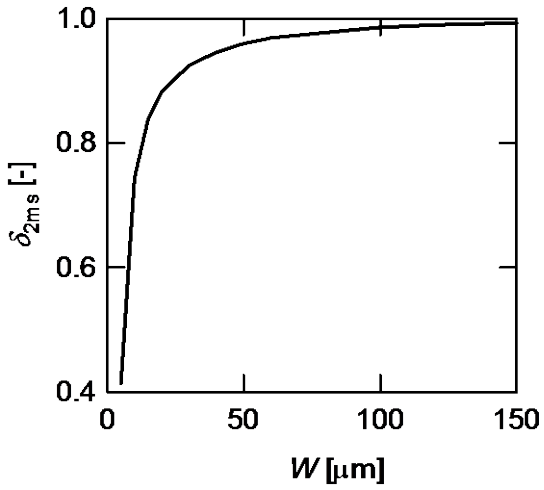

Fig. 4. δ_{2ms} as function of fluid segment size W for MLmixer.

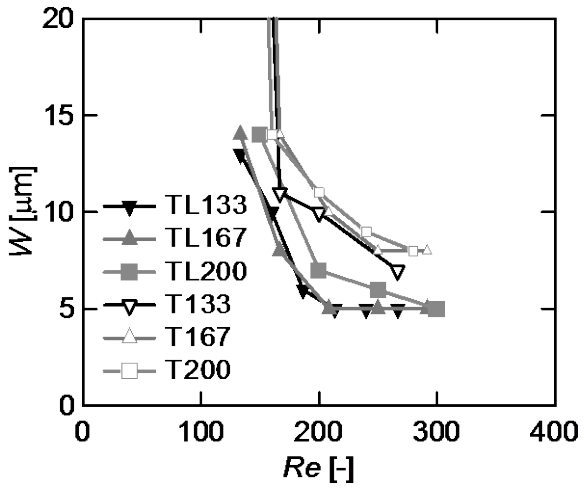

Fig. 5. Relationship between effective fluid segment size and Reynolds number.

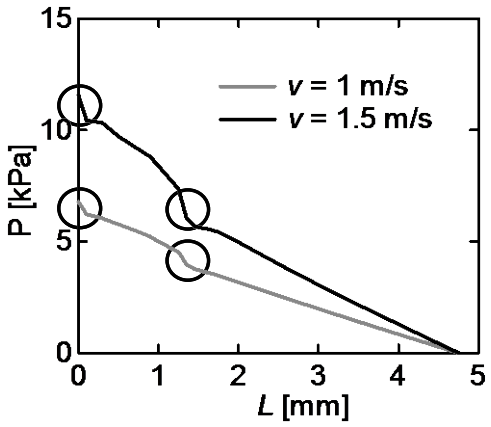

Fig. 6. Static pressure of TL167. The plane right after channel confluence is defined as L = 0 mm, and the plane right before channel bend is defined as L = 1 mm. The pressure at the channel outlet is set at 0 kPa as the reference.

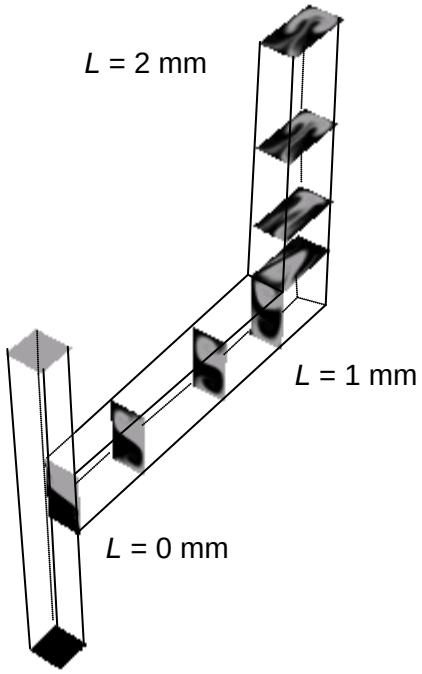

Fig. 7. Profiles of mass fraction of A inside TL167 (v = 1 m/s).

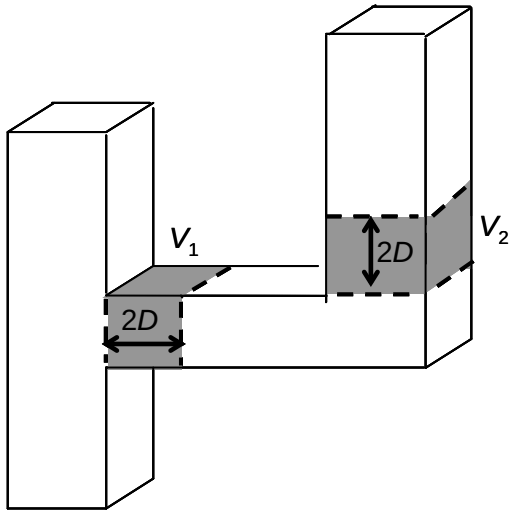

Fig. 8. Focused space of TLmixer used to obtain energy dissipation rate.

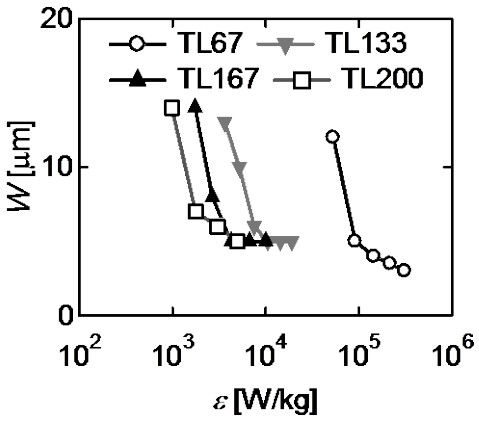

Fig. 9. Relationship between effective fluid segment size and energy dissipation rates.

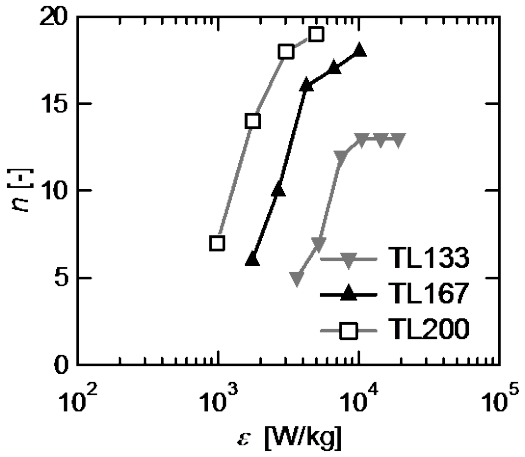

Fig. 10. Relationship between split number and energy dissipation rate.

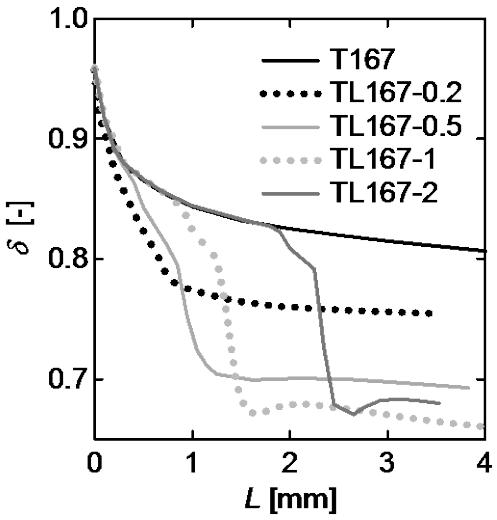

Fig. 11 Influence of distance *X* between channel confluence and bend (v = 1 m/s).

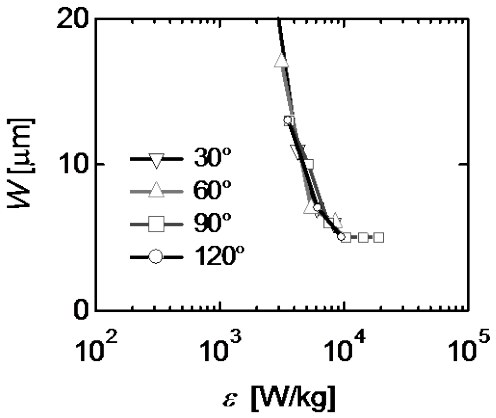

Fig. 12. Influence of bend angle θ on effective fluid segment size.

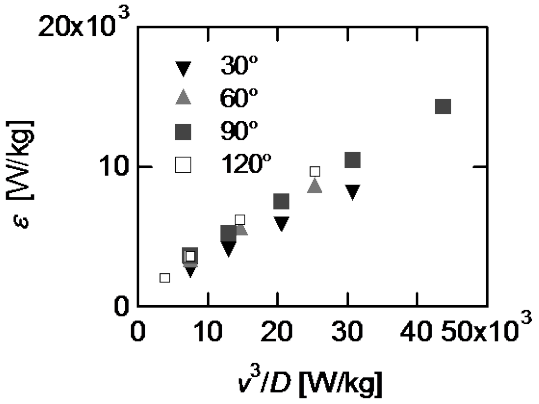

Fig. 13. Plots of ε against v^3/D used to obtain f^*.

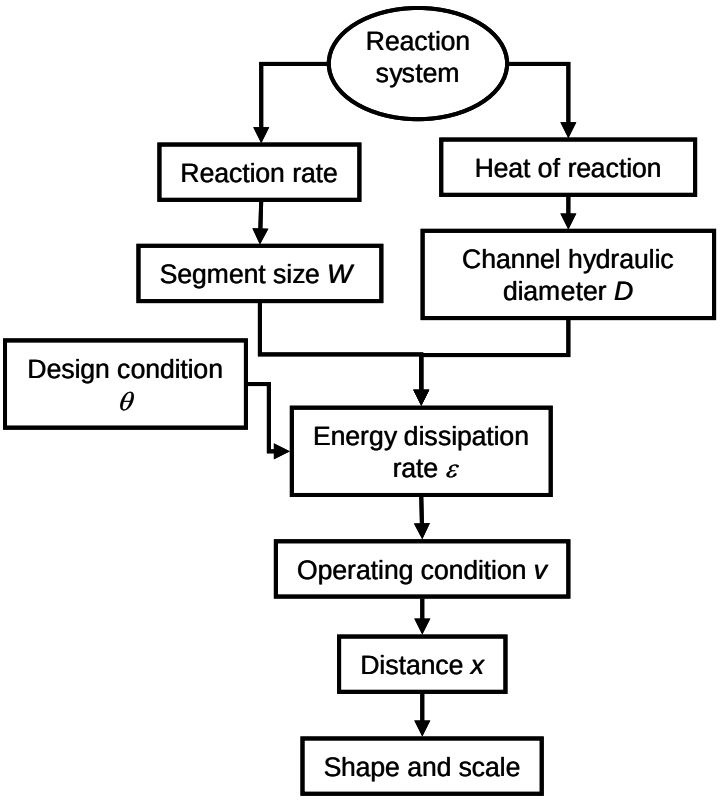

Fig. 14. Design procedure for micromixer.